

ARTICLES

Explosive Desorption and Fragmentation of Molecular Ion from Solid Fullerene by Intense Nonresonant Femtosecond Laser Pulses

Tomoyuki Yatsunami* and Nobuaki Nakashima

*Department of Chemistry, Graduate School of Science, Osaka City University, 3-3-138 Sugimoto, Sumiyoshi, Osaka 558-8585 Japan**Received: March 17, 2008; Revised Manuscript Received: April 22, 2008*

Desorption of C_{60}^+ and its dimer cation was investigated on irradiation with nonresonant femtosecond laser pulses at 1.4 μm . Ionization of solid C_{60} revealed strikingly different features, such as the absence of multiply charged molecular ions, the emission of C^+ at low laser intensity, C_2 attachments, delayed ionization, and dimer cation formation, as compared with the gas phase experiments. The large kinetic energy distribution of ions found in this study indicated that the desorption process was mainly driven by an electrostatic mechanism rather than by thermal, photochemical, or volume expansion mechanisms. Singly charged C_{60} emission by a Coulomb explosion due to the high density of C_{60}^+ is suggested.

Introduction

Mass spectrometry by ion desorption¹ is widely used in chemistry, biology, and medicine for qualitative analysis of materials. The success of intact molecular (parent) ion detection by MALDI (matrix assisted laser desorption ionization)² and DIOS (desorption ionization on porous silicon)³ provides many advantages for analytical purposes. Despite the importance of intact ion detection in those methods, controversy as to the ionization and desorption mechanism is ongoing. The complexity is due in part to the contribution of the matrix and substrate in the processes. The ablation processes of metals and polymers where bond breaking should be involved have also been extensively studied.⁴ One of the difficulties in clarifying the mechanism for all the desorption processes mentioned above is the absence of gas phase experiments of the isolated condition. On the other hand, intact ion formation⁵ in addition to highly charged molecular ion formation⁶ in the gas phase by using femtosecond laser pulses was identified. A variety of laser parameters, such as wavelength, pulse duration, and polarization,⁷ have been examined for the formation of intact molecular ions. A key issue is that fragmentation is enhanced when the cation radical exhibits absorption at the laser wavelength, although the ion was formed by a nonresonant ionization process of neutral molecules. In addition, it is clear that a shorter duration pulse is better to avoid fragmentation.⁸ Investigation of the direct ionization/desorption mechanism for producing intact molecular ions from solid samples will allow a femtosecond laser as a useful tool for mass spectrometry and will also provide important information to help in the understanding of other desorption processes.

However, the main focus of most femtosecond laser ionization studies has been isolated atoms, molecules, and clusters. A representative molecule in intense light field chemistry⁹ is the fullerene molecule (C_{60}), and many femtosecond laser ionization

experiments have been reported in the gas phase.¹⁰ Multiply charged C_{60} up to 12^+ was observed with 70 fs pulse irradiation at an off-resonant wavelength of the cation radical in the gas phase.¹¹ On the other hand, C_{60} was broken down completely to highly charged carbons by a Coulomb explosion¹² under ultraintense laser fields.¹³ Recently, solid C_{60} deposited on a silicon substrate was ionized with a femtosecond laser, which was in resonance with the substrate and also with the neutral and cationic states of the C_{60} (800 nm, 120 fs; 400 nm, ~ 200 fs).¹⁴ However, the femtosecond ionization and desorption mechanism of C_{60} has not yet been made clear. To avoid the complexity that arises from postionization processes initiated by photo absorption of the cation radical¹⁵ as well as from substrate heating or ionization processes, we investigated the direct (that is, with neither a prevaporization laser nor a matrix, but with a thick organic layer and a transparent substrate) nonresonant femtosecond laser ionization and desorption of solid C_{60} .¹⁶ Because organic molecules in the solid phase are aggregated by van der Waals force, the electronic character of the molecule remains. Therefore, the character of the isolated molecule will be reflected in the ionization and fragmentation processes of the solid. Comparison with experiments in the gas phase will provide fruitful information toward understanding the ionization and desorption mechanism.

Experimental Methods

An excess amount of C_{60} (Aldrich, 99.95 %) was finely powdered by stirring in toluene for several hours, and the slurry was deposited on a quartz plate, followed by solvent evaporation in a vacuum. Details of the ionization experiments have been described elsewhere.¹⁷ Briefly, the ion generated by focusing laser light was analyzed by a homemade Wiley–McLaren-type dual extraction stage time-of-flight mass spectrometer with resolution ($m/\Delta m$, fwhm) of 500 at $m/z = 129$ for xenon. An aperture of 6 mm diameter was located on the extraction plate. The base pressure of both the ionization and time-of-flight chambers was below 5×10^{-7} Pa. The pressure during the C_{60}

* To whom correspondence should be addressed. Telephone: +81-6-6605-2554. Fax: +81-6-6605-2522. E-mail: tomo@sci.osaka-cu.ac.jp.

experiments was below 10^{-5} Pa. A thin sample plate was inserted in the acceleration region, and hence, the ion optics were optimized to correct the distortion of the electro static field. The sample plate was moved to the shooting laser beam on the fresh surface. A 45 fs pulse from a 0.5 TW all-diode-laser-pumped Ti:sapphire laser system (Thales laser, α 100/XS, 100 Hz, > 15 mJ, 800 nm) was used to pump an optical parametric amplifier (Quantronix, TOPAS). The pulse width was measured by a second-order scanning autocorrelator (APE, PulseCheck). The same optical elements, such as the ionization chamber window, focusing lens, beam splitter, and neutral density filter, were placed in front of the autocorrelator to have the same group velocity dispersion. A pulse of 58 fs (fwhm, Sech²) duration at $1.4 \mu\text{m}$ was used for the experiments. The direction of the laser polarization was orthogonal to the time-of-flight axis. The laser beam was focused onto the C_{60} with an incident angle of 45 degrees using a planoconvex quartz lens with a focusing length of 300 mm. The actual laser intensity at the focus was determined by measuring the saturation intensity, I_{sat} , of xenon by the method of Hankin et al.¹⁸ The output signal from an MCP was averaged by a digital oscilloscope, and the ion yield was obtained by integrating over the appropriate peak in the time-of-flight spectrum.

Results and Discussion

Figure 1 shows the time-of-flight mass spectra of C_{60} . Intact C_{60}^+ was observed below $5 \times 10^{12} \text{ W cm}^{-2}$. As the laser intensity increased, C^+ and a series of C_2 loss fragments (C_{60-2n}^+) appeared. The relatively broad width of the C_{60}^+ peak ($\Delta m \sim 14$, fwhm; isotope peaks were not resolved; Figure 1a) and its C_2 loss fragment ions indicated that C_{60}^+ gained a large amount of kinetic energy. The peak width (fwhm) of C^+ and C_{60}^+ at $8.5 \times 10^{12} \text{ W cm}^{-2}$ was equivalent to the kinetic energy distribution of ~ 3 and 7 eV, respectively (Figure 2). The kinetic energy distribution of water (gas) was only 0.03 eV measured with the same spectrometer; thus, the instrumental response was considered negligibly small. The large kinetic energy of ions indicated that the origins of C^+ emissions are likely not an ordinary thermally induced chemical bond-breaking reaction, but a kind of repelling of atoms by a strong electrostatic force, such as a Coulomb explosion. The broad width also reflected the high vibrational temperature of the ions.

Significant fragmentation, the tailing component of C_{60}^+ attributable to delayed ionization,¹⁹ and $(\text{C}_{60})_2^+$ formation became visible at higher intensities in addition to the splitting and broadening of some fragment peaks (Figure 1 b). Due to the broadness of the peak, it was not clear whether $(\text{C}_{60})_2^+$ was a single peak or composed of several peaks due to coalescence (C_2 attachment and detachment products of fused C_{120}).²⁰ Attachments of C_2 to C_{60}^+ (C_{60+2n}^+), such as C_{64}^+ ($m/z = 768$) and C_{66}^+ ($m/z = 792$), were identified (Figure 2), but the tailing component of C_{60}^+ masked C_{62}^+ ($m/z = 744$). The C_2 attached ions were masked by the delayed ionization component and not recognized above $10 \times 10^{12} \text{ W cm}^{-2}$. Contrary to the results of 400 nm ionization of solid C_{60} on a silicon substrate,¹⁴ $1.4 \mu\text{m}$ ionization of solid C_{60} on a quartz substrate revealed strikingly different features, such as the ejection of C^+ at low laser intensity (Figure 1a) and the absence of C_{60}^{2+} (Figure 1c). The ion yield of $(\text{C}_{60})_2^+$ increased as the laser intensity increased in this study, whereas it diminished at high intensity on a silicon substrate.¹⁴ These differences indicated that there were different ionization and desorption mechanisms, depending on the laser and sample conditions. The effect of the substrate should be important if the thickness of the adsorber is thin enough to allow

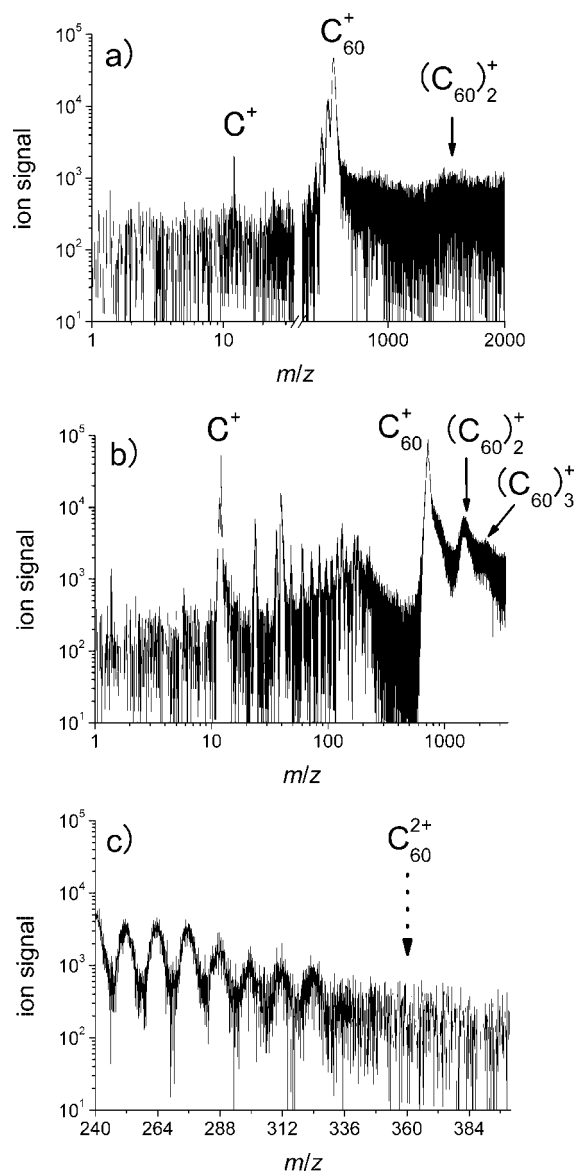


Figure 1. Time-of-flight mass spectra of solid C_{60} at different intensities (1.4 mm , 58 fs): (a) $8.5 \times 10^{12} \text{ W cm}^{-2}$, (b) $13 \times 10^{12} \text{ W cm}^{-2}$, and (c) $11 \times 10^{12} \text{ W cm}^{-2}$.

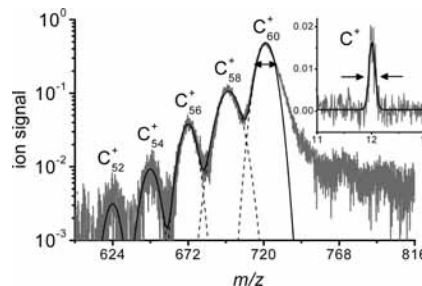


Figure 2. Time-of-flight mass spectrum of solid C_{60} at $8.5 \times 10^{12} \text{ W cm}^{-2}$ (1.4 mm , 58 fs). Inset shows the same mass spectra of C^+ . Dashed and solid lines indicate Gaussian fit of each mass peak and the sum of them. Arrows indicate the full width at half maximum of C^+ and C_{60}^+ peaks, respectively.

the laser beam to penetrate the substrate. In such a case, the substrate would be excited and heated because the band gap of silicon (1.1 eV corresponds to $1.1 \mu\text{m}$) is lower than that of C_{60} . Substrate would be ionized at a lower laser intensity as compared with C_{60} , and plasma may contribute to the whole process when the laser intensity is sufficiently high. In addition,

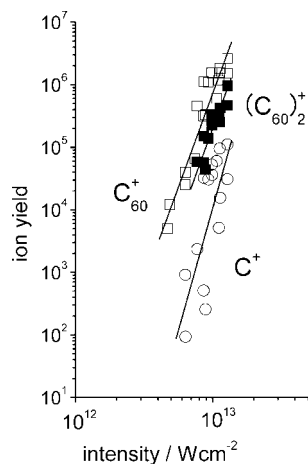


Figure 3. Ion yields of C_{60}^+ (open square), $(C_{60})_2^+$ (solid square), and C^+ (open circle) as a function of laser intensity. The solid lines have a slope of 6 (C_{60}^+ and $(C_{60})_2^+$) and 8 (C^+).

the contribution of the photoinduced fragmentation process of C_{60}^+ must be included because the molar absorption coefficient of cation radical at 400 nm was approximately 40 times larger than that at 1.4 μm ,²¹ and the relatively long duration of the laser pulse (200 fs) was sufficient to excite the cation radical. Although the benefit of the substrate effect has been shown by DIOS-MS as an intact molecular ion formation method,³ to investigate C_{60} alone, it is necessary to prevent the substrate from affecting the processes. The results for C_{60} can be compared with those of direct ionization/desorption experiments that use free electron lasers (FEL, 8.8 μm , 2 μs , NaCl substrate).²² The results with the FEL laser (long duration and infrared pulses) are obviously dominated by thermal processes. Similar behavior, such as the dominance of C_{60}^+ , attachments of C_2 to C_{60}^+ , and delayed ionization, was observed in our experiments. In the gas phase, only the longer-duration laser pulse (longer than a picosecond) resulted in violent fragmentation and delayed ionization.²³ Neither attachments of C_2 nor dimer cation formation were reported in the gas phase by short-duration pulse irradiation. From these facts, we can conclude that desorption of solid C_{60} by femtosecond laser pulses was influenced by thermal effects, although 58 fs pulses were used in this study.

Figure 3 shows the laser intensity dependence of C_{60} ion yields. The slopes indicated in Figure 3 are 6 for C_{60}^+ and $(C_{60})_2^+$ and 8 for C^+ . The ionization rate depends mainly on the ionization potential; however, it differs by the depth from the surface in the case of a solid. Because the laser pulses penetrate into the bulk solid, the broad distribution of ionization potential should be taken into account. However, the contribution of the surface would be significant only in the case of a nanosize particle and, thus, could be neglected for our fairly large particle sample. The ionization potentials of organic solids have been studied in detail by Sato et al.²⁴ The vertical and adiabatic ionization potentials of C_{60} are 7.61 eV in the gas phase, whereas the work function, threshold (bulk), and peak (near to the surface) ionization potentials of solid C_{60} are 4.85, 6.17, and 6.85 eV, respectively.²⁵ They correspond to 6, 7, and 8 photons of a 1.4 μm pulse (0.89 eV). The Keldysh adiabaticity parameter γ defines the border between the multiphoton ionization and tunnel ionization regime of atoms.²⁶ According to the photoelectron measurements of C_{60} in the gas phase, tunnel ionization took place above $10^{14} \text{ W cm}^{-2}$ ($\gamma = 0.80$, 800 nm).²⁷ Suppose the ionization potential is 6.17 eV, then γ is 1.3 at $1 \times 10^{13} \text{ W cm}^{-2}$ (1.4 μm). Under our experimental

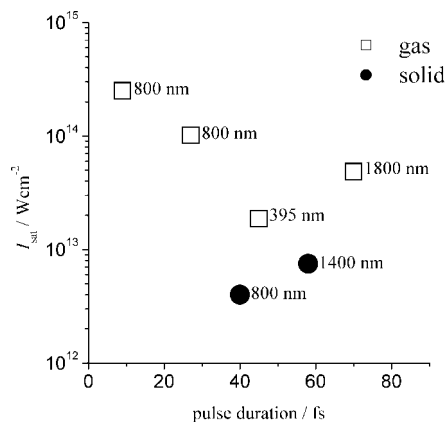


Figure 4. Saturation intensities, I_{sat} , of C_{60}^+ as a function of pulse duration. Earlier experiments (squares, 1800 nm, 710 fs, ref 11; 800 nm, 9 and 27 fs, ref 10; 395 nm, 45 fs refs 10 and 37) in the gas phase and the present experiments in the solid phase (circles) are compared.

conditions, both tunneling and multiphoton ionization mechanisms may be involved. Figure 4 compares the saturation intensity, I_{sat} , of C_{60}^+ . I_{sat} corresponds to the intensity at a certain ionization probability, which in turn depends on the ionization potential, wavelength, and pulse duration. I_{sat} is defined as the point at which the ion yield (linear scale), extrapolated from the high-intensity linear portion of the curve, intersects the intensity axis (logarithmic scale).¹⁸ Solid C_{60} needs 1 order of magnitude smaller intensity than in the gas phase to be ionized. The significant difference may originate mainly in their ionization potentials; however, comparison with theoretical model is difficult due to heavy fragmentation at high intensity.

The absence of multiply charged molecular ions at high laser intensity and the presence of C^+ at low laser intensity were strikingly different features of the solid phase as compared with the gas phase experiments. These features should be key clues for clarifying the desorption processes. Neutral C_2 emission occurred; however, C^+ ion production by the dissociation and ionization of C_2 was not considered because the pulse duration of the laser is much shorter than the time scale of the dissociation process of neutral fragment. It should be mentioned that C_{60}^{2+} was absent also in the 800 nm ionization experiments of solid, even above $10^{14} \text{ W cm}^{-2}$ (not shown). Highly charged molecular ions have been commonly observed from many organic systems by femtosecond laser irradiation in the gas phase.²⁸ Up to a 12+ fullerene was observed experimentally,¹¹ and its stability was theoretically proved.²⁹ Even in the solid phase, highly charged molecular ions must initially be formed by 1.4 μm (58 fs) pulse irradiation. Once highly charged C_{60} was formed, redistribution of charges was presumably completed in a very short time because of the high density of the solid. Gas phase experiments have been performed under a typical pressure of $5.0 \times 10^{-5} \text{ Pa}$, which corresponds to $2.0 \times 10^{-11} \text{ M}$; therefore, charge redistribution is not possible. In contrast, the concentration of C_{60} in the solid phase is 2.3 M (1.69 g cm^{-3}), and thus, hole neutralization by neighboring neutral and lower charge states of C_{60} would take place immediately, finally resulting only in the C_{60}^+ formation.

The formation of C_{60}^+ and C_{60}^{2+} without fragmentation was reported in collisional charge transfer experiments between C_{60}^{z+} ($z = 1-5$) and neutral C_{60} in the gas phase.³⁰ Thus, the charge transfer reaction itself will not cause fragmentation under the isolated conditions. On the other hand, neutralization of highly charged C_{60} by neighboring molecules should release consider-

able energy to the lattice in the solid phase. This process could produce electronically excited states of ions with excess energy. The amount of energy released could be estimated from the results of the investigation of a multiply charged C_{60} dimer.³¹ For example, the difference in interaction energy between $(C_{60})_2^{4+}$ and $(C_{60})_2^{2+}$ at the fixed intermolecular distance of 9.5 Å was ~ 4 eV. The experimental kinetic energy release from dimer dissociation ($(C_{60})_2^{4+}$ to $2C_{60}^{2+}$) indicated the internal excitation of the monomer was ~ 2.8 eV.³¹ A conformational change might occur through the charge transfer process in a real solid system, and a significant amount of energy could be expected to be transferred to the lattice. The electron–hole recombination would also produce significant excess energy. In addition to these processes, some of the electrons will penetrate into the bulk and also contribute to heat the lattice, although most of the electrons will be ejected from the surface. In fact, delayed (thermal) ionization was observed at higher intensity. The tailing component of C_{60}^+ (Figure 1b) can clearly be attributed to the delayed ionization, with its decay of 4 μ s fitted by the first order at 11×10^{12} W cm⁻². Due to insufficient resolution, we cannot fit the decay using the power law.³² The appearance of delayed ionization is not so surprising, because desorption takes longer than the pulse duration so that some time will be available for energy redistribution and thermalization. The super thermal (vibrationally excited) condition would cause fragmentation. One may consider delayed ejection because not every ion was desorbed from the uppermost layer. However, delayed ejection (penetration effect) would not be serious because the focusing diameter and surface roughness in this experiment was on the order of a few tens of micrometers. The delayed ejection will not affect our results, but such an effect would be important for metals with very clean surfaces.

There presumably could be a low probability of photoinduced fragmentation of the cation radical at 1.4 μ m excitation because C_{60} is transparent at the laser wavelength and its cation radical has little absorption. The molar absorption coefficient of the cation radical at 1.4 μ m was about 1/10 that at 0.8 μ m, as measured by electrochemical oxidation in solution.²¹ Furthermore, the contribution of the photoinduced fragmentation process was negligible at excitation wavelengths longer than 1.5 μ m in the gas phase.³³ However, photoinduced decomposition of a dimer cation would occur if the dimer cation staying in the solid has strong absorption at the laser wavelength of 1.4 μ m, even with a very short pulse.³⁴ The very broad width of $(C_{60})_2^+$ (Δm was ~ 200) could be attributed to the collisional formation from neutral C_{60} and ions thermally emitted from the surface. A dimer cation was presumably formed away from the surface by the collision at the wing of the laser focus spot where neutral C_{60} remains, giving a mass peak with broad distribution. The photodissociation of dimer ejected from the surface was not considered because the pulse duration of the laser is much shorter than the time scale of the desorption process. The same laser intensity dependence with monomer ion could be explained. The activation energy of $(C_{60})_2^+$ dissociation is 0.372 eV;³⁵ therefore, the internal energy should be lower than this value under the assumption of the weakly bonded dimer of $(C_{60})_2^+$. Therefore, we have to assume a covalently bonded dimer formed by reaction with the solid $C_{60}(s)$.

We postulated that the desorption process by femtosecond laser pulses was driven by an electrostatic mechanism rather than by a thermal (melting and boiling), photochemical (bond-breaking), or volume expansion mechanism due to the large kinetic energy of ions. Singly charged C_{60} was emitted by a Coulomb explosion due to the high density of C_{60}^+ produced

by the sequential charge redistribution of the initially formed highly charged ions. On the assumption that the intermolecular distance is 9.5 Å, the Coulombic repulsion energy between $C_{60}^+(s)$ is 1.5 eV. If C_{60}^+ is surrounded by several $C_{60}^+(s)$, the energy will be well above the enthalpy of neutral C_{60} sublimation (1.9 eV).³⁶ C^+ would also be emitted by Coulomb explosion, probably due to the temporal charge localization³⁷ within the framework of C_{60} . Although bond breaking is necessary, the Coulomb explosion mechanism is also proposed for ion ejection from inorganic crystals³⁸ and graphite.³⁹ The above Coulomb explosion desorption mechanism of C_{60} might be one candidate. However, it is notable that C_{60} is somewhat a special molecule due to its stability in multiply charged states and its large dissociation energy. Further examinations of a variety of organic molecules are necessary to draw a decisive conclusion about the general ionization and desorption mechanism by femtosecond laser pulses, and reducing the kinetic energy of ions is a key issue for high resolution mass spectroscopy.

Acknowledgment. The present research was supported in part by a Grant-in-aid from the Ministry of Education, Culture, Sports, Science and Technology, Japan.

References and Notes

- (1) Busch, K. L. *J. Mass Spectrom.* **1995**, *30*, 233.
- (2) (a) Karas, M.; Hillenkamp, F. *Anal. Chem.* **1988**, *60*, 2299. (b) Tanaka, K.; Waki, H.; Ido, Y.; Akita, S.; Yoshida, Y.; Yoshida, T. *Rapid Commun. Mass Spectrom.* **1988**, *2*, 151–153.
- (3) Wei, J.; Buriak, J. M.; Siuzdak, G. *Nature* **1999**, *399*, 243.
- (4) Bäuerle, D. *Laser Processing and Chemistry*; Springer: Berlin, 2000.
- (5) DeWitt, M. J.; Levis, R. J. *J. Chem. Phys.* **1995**, *102*, 8670.
- (6) Ledingham, K. W. D.; Singhal, R. P.; Smith, D. J.; McCanny, T.; Graham, P.; Kilic, H. S.; Peng, W. X.; Wang, S. L.; Langley, A. J.; Taday, P. F.; Kosmidis, C. *J. Phys. Chem. A* **1998**, *102*, 3002.
- (7) (a) Nakashima, N.; Yatsuhashi, T.; Murakami, M.; Mizoguchi, R.; Shimada, Y. In *Advances in Multiphoton Processes and Spectroscopy*; Lin, S.H., Villaeys, A.A., Fujimura, Y. Eds.; World Scientific Pub. Co Inc: Singapore, 2006; Vol. 17, p 179. (b) Nakashima, N.; Yatsuhashi, T. In *Progress in Ultrafast Intense Laser Science II*; Yamanouchi, K., Chin, S. L., Agostini, P., Ferrante, G. Eds.; Springer: Berlin, 2007; p 25.
- (8) Tanaka, M.; Panja, S.; Murakami, M.; Yatsuhashi, T.; Nakashima, N. *Chem. Phys. Lett.* **2006**, *427*, 255.
- (9) (a) Yamanouchi, K. *Science* **2002**, *295*, 1659. (b) Nakashima, N.; Shimizu, S.; Yatsuhashi, T.; Sakabe, S.; Izawa, Y. *J. Photochem. Photobiol. C* **2000**, *1*, 131.
- (10) (a) Shchatsin, I.; Laermann, T.; Stibenz, G.; Steinmeyer, G.; Stalmashonak, A.; Zhavoronkov, N.; Schulz, C. P.; Hertel, I. V. *J. Chem. Phys.* **2006**, *125*, 194320. (b) Hertel, I. V.; Laermann, T.; Schulz, C. P. *Adv. At. Mol. Opt. Phys.* **2005**, *50*, 219.
- (11) Bhardwaj, V. R.; Corkum, P. B.; Rayner, D. M. *Phys. Rev. Lett.* **2003**, *91*, 203004.
- (12) Shimizu, S.; Zhakhovskii, V.; Sato, F.; Okihara, S.; Sakabe, S.; Nishihara, K.; Izawa, Y.; Yatsuhashi, T.; Nakashima, N. *J. Chem. Phys.* **2002**, *117*, 3180.
- (13) Kou, J.; Zhakhovskii, V.; Sakabe, S.; Nishihara, K.; Shimizu, S.; Kawato, S.; Hashida, M.; Shimizu, K.; Bulanov, S.; Izawa, Y.; Kato, Y.; Nakashima, N. *J. Chem. Phys.* **2000**, *112*, 5012.
- (14) (a) Kobayashi, T.; Kato, T.; Matsuo, Y.; Kurata-Nishimura, M.; Kawai, J.; Hayashizaki, Y. *J. Chem. Phys.* **2007**, *126*, 061101. (b) Kobayashi, T.; Kato, T.; Matsuo, Y.; Kurata-Nishimura, M.; Hayashizaki, Y.; Kawai, J. *J. Chem. Phys.* **2007**, *127*, 111101.
- (15) (a) Harada, H.; Shimizu, S.; Yatsuhashi, T.; Sakabe, S.; Izawa, Y.; Nakashima, N. *Chem. Phys. Lett.* **2001**, *342*, 563. (b) Harada, H.; Tanaka, M.; Murakami, M.; Shimizu, S.; Yatsuhashi, T.; Nakashima, N.; Sakabe, S.; Izawa, Y.; Tojo, S.; Majima, T. *J. Phys. Chem. A* **2003**, *107*, 6580. (c) Trushin, S. A.; Fuß, W.; Schmid, W. E. *J. Phys. B* **2004**, *37*, 3987. (d) Wu, D.; Wang, Q.; Cheng, X.; Jin, M.; Li, X.; Hu, Z.; Ding, D. *J. Phys. Chem. A* **2007**, *111*, 9494. (e) Pearson, B. J.; Nichols, S. R.; Weinacht, T. *J. Chem. Phys.* **2007**, *127*, 131101.
- (16) Shimizu, S.; Hashida, M.; Murakami, M.; Yatsuhashi, T.; Nakashima, N.; Sakabe, S. *Abstracts of Papers, International Symposium on Atoms, Molecules, and Clusters in Intense Laser Fields 2*; Tokyo, Japan, 2005; p 29.
- (17) Yatsuhashi, T.; Obayashi, T.; Tanaka, M.; Murakami, M.; Nakashima, N. *J. Phys. Chem. A* **2006**, *110*, 7763.

- (18) Hankin, S. M.; Villeneuve, D. M.; Corkum, P. B.; Rayner, D. M. *Phys. Rev. A* **2001**, *64*, 013405.
- (19) (a) Campbell, E. E. B.; Ulmer, G.; Hertel, I. V. *Phys. Rev. Lett.* **1991**, *67*, 1986. (b) Wurz, P.; Lykke, K. R. *J. Chem. Phys.* **1991**, *95*, 7008.
- (20) Yerezian, C.; Hansen, K.; Diederich, F.; Whetten, R. L. *Nature* **1992**, *359*, 44.
- (21) Webster, R. D.; Heath, G. A. *Phys. Chem. Chem. Phys.* **2001**, *3*, 2588.
- (22) Hamada, Y.; Kondoh, H.; Ogawa, Y.; Tono, K.; Ohta, T.; Ogi, Y.; Endo, T.; Tsukiyama, K.; Kuroda, H. *Jpn. J. Appl. Phys.* **2002**, *41*, 113.
- (23) Campbell, E. E. B.; Hansen, K.; Hoffmann, K.; Korn, G.; Tchapyguine, M.; Wittmann, M.; Hertel, I. V. *Phys. Rev. Lett.* **2000**, *84*, 2128.
- (24) (a) Sato, N.; Seki, K.; Inokuchi, H. *J. Chem. Soc., Faraday Trans. 2* **1981**, *77*, 1621. (b) Sato, N. In *Electrical and Related Properties of Organic Solids*; Munn, R. W., Miniewicz, A., Kuchta, B. Eds.; Springer: Netherlands, 1997; p 157.
- (25) Sato, N.; Saito, Y.; Shinohara, H. *Chem. Phys.* **1992**, *162*, 433.
- (26) Keldysh, L. V. *Sov. Phys. JETP* **1965**, *29*, 1307.
- (27) Campbell, E. E. B.; Hoffmann, K.; Rottke, H.; Hertel, I. V. *J. Chem. Phys.* **2001**, *114*, 1716.
- (28) (a) Murakami, M.; Mizoguchi, R.; Shimada, Y.; Yatsuhashi, T.; Nakashima, N. *Chem. Phys. Lett.* **2005**, *403*, 238. (b) Yatsuhashi, T.; Nakashima, N. *J. Phys. Chem. A* **2005**, *109*, 9414.
- (29) (a) Sahnoun, R.; Nakai, K.; Sato, Y.; Kono, H.; Fujimura, Y.; Tanaka, M. *Chem. Phys. Lett.* **2006**, *460*, 167. (b) Sahnoun, R.; Nakai, K.; Sato, Y.; Kono, H.; Fujimura, Y.; Tanaka, M. *J. Chem. Phys.* **2006**, *125*, 184306.
- (30) Cederquist, H.; Hvelplund, P.; Lebius, H.; Schmidt, H. T.; Tomita, S.; Huber, B. A. *Phys. Rev. A* **2001**, *63*, 025201.
- (31) Zettergren, H.; Schmidt, H. T.; Reinhard, P.; Cederquist, H.; Jensen, J.; Hvelplund, P.; Tomita, S.; Manil, B.; Rangama, J.; Huber, B. A. *J. Chem. Phys.* **2007**, *126*, 224303.
- (32) Hansen, K.; Echt, O. *Phys. Rev. Lett.* **1997**, *78*, 2337.
- (33) Bhardwaj, V. R.; Corkum, P. B.; Rayner, D. M. *Phys. Rev. Lett.* **2004**, *93*, 043001.
- (34) (a) Murakami, M.; Tanaka, M.; Yatsuhashi, T.; Nakashima, N. *J. Chem. Phys.* **2007**, *126*, 104304. (b) Tanaka, M.; Panja, S.; Murakami, M.; Yatsuhashi, T.; Nakashima, N. *Chem. Phys. Lett.* **2006**, *427*, 255.
- (35) Branz, W.; Malinowski, N.; Enders, A.; Martin, T. P. *Phys. Rev. B* **2002**, *66*, 094107.
- (36) Piacente, V.; Gigli, G.; Scardala, P.; Giustini, A. *J. Phys. Chem.* **1995**, *99*, 14052.
- (37) Yatsuhashi, T.; Murakami, M.; Nakashima, N. *J. Chem. Phys.* **2007**, *126*, 194316.
- (38) Henyk, M.; Wolframm, D.; Reif, J. *Appl. Surf. Sci.* **2000**, *168*, 263.
- (39) Kaplan, A.; Lenner, M.; Palmer, R. E. *Phys. Rev. B* **2007**, *76*, 073401.
- (40) Tchapyguine, M.; Hoffmann, K.; Dühr, O.; Hohmann, H.; Korn, G.; Rottke, H.; Wittmann, M.; Hertel, I. V.; Campbell, E. E. B. *J. Chem. Phys.* **2000**, *112*, 2781.

JP8023028